THE ASTROPHYSICAL JOURNAL, 443:514–526, 1995 April 20

ROSAT OBSERVATIONS OF COMPACT GROUPS OF GALAXIES

RACHEL A. PILDIS AND JOEL N. BREGMAN
Department of Astronomy, University of Michigan, Ann Arbor, MI 48109-1090;
pildis,jbregman@astro.lsa.umich.edu

AND

AUGUST E. EVRARD
Department of Physics, University of Michigan, Ann Arbor, MI 48109-1120;
evrard@umich.edu

Received 1994 July 28; accepted 1994 October 27

ABSTRACT

We have systematically analyzed a sample of 13 new and archival *ROSAT* Position Sensitive Proportional Counter observations of compact groups of galaxies: 12 Hickson compact groups plus the NCG 2300 group. We find that approximately two-thirds of the groups have extended X-ray emission and, in four of these, the emission is resolved into diffuse emission from gas at a temperature of $kT \sim 1$ keV in the group potential. All but one of the groups with extended emission have a spiral fraction of less than 50%. The baryon fraction of groups with diffuse emission is 5%–19%, similar to the values in clusters of galaxies. However, with a single exception (HCG 62), the gas-to-stellar mass ratio in our groups has a median value near 5%, somewhat greater than the values for individual early-type galaxies and two orders of magnitude than in clusters of galaxies. The X-ray luminosities of individual group galaxies are comparable to those of similar field galaxies, although the L_X-L_B relation for early-type galaxies may be flatter in compact groups than in the field.

Subject headings: diffuse radiation — galaxies: clusters: general — X-rays: galaxies

1. INTRODUCTION

Poor groups of galaxies have been studied much less than have rich clusters, even though they are the most common type of galaxy grouping and thus are more likely to be representative of the universe as a whole than relatively rare clusters. In large part, this is because groups are much more difficult to identify: they have very few galaxies and tend to have small overdensities relative to the background. Even those groups selected by "objective" searches through redshift space such as the CfA groups (Huchra & Geller 1982) may not all be gravitationally bound (Moore, Frenk, & White 1993). These concerns lead one to search for groups with few galaxies that nonetheless have relatively large overdensities for easy identification; such groups do exist — compact groups of galaxies.

Compact groups contain some of the densest concentrations of galaxies known, with galaxy densities comparable to or greater than even those of the cores of rich clusters. These groups typically contain fewer than 10 members, and the galaxy–galaxy separations are on the order of a galaxy diameter. The high densities would imply that these are ideal laboratories for studying galaxy interactions and merging.

One well-studied sample of compact groups is the Hickson compact groups (HCGs) as defined by Hickson (1982). Spectroscopy and imaging have shown that most of the groups consist of galaxies with concordant redshifts (Hickson et al. 1992) and that many of these galaxies display signs of interaction such as tidal tails and distorted spiral arms (Mendes de Oliveria & Hickson 1994; Rubin, Hunter, & Ford 1991). However, studies of early-type galaxies in HCGs find them to be less boxy than field ellipticals (Fasano & Bettoni 1994; Zepf & Whitmore 1993), which might imply that these galaxies have undergone fewer interactions than have field ellipticals.

The question of the interaction history of HCGs is not answered by studies at radio and IR frequencies. Several investigations into the neutral hydrogen distribution in various HCGs (Shostak, Sullivan, & Allen 1984; Williams & van Gorkom 1988; Williams, McMahon, & van Gorkom 1991) have shown that some of the more compact groups have H I clouds that encompass entire groups, while the less compact groups have H I confined to the (spiral) galaxies. The galaxies in these latter groups contain only half the neutral hydrogen that similar galaxies in loose groups have (Williams & Rood 1987). Hickson et al. (1989) found that the *IRAS* far-IR (FIR) emission in compact groups was enhanced, but this was disputed by Sulentic & Mello Rabaça (1993). Moles et al. (1994) considered 25 μm emission in addition to FIR emission and found no enhancement over the levels seen in isolated pairs of galaxies.

One can determine that a group is gravitationally bound by detecting hot gas in the group potential well via X-ray observations. Few such observations of compact groups have been made, but this situation is rapidly changing. Bahcall, Harris, & Rood (1984) observed four HCGs (and an additional Arp group) with the *Einstein* X-ray telescope and found extended emission in HCG 92 (Stephan's Quintet) and Arp 330. The sensitivity to emission at temperatures near 1 keV of the *ROSAT* X-ray telescope has made possible a great number of observations of compact groups of galaxies, two of which have already been reported upon in the literature. HCG 62 was found to be a bright source of diffuse X-rays by Ponman & Bertram (1993), and the NGC 2300 group of galaxies was found to have extended X-ray emission by Mulchaey et al. (1993). The latter paper claimed that the NGC 2300 group has a baryon fraction of only 4% (although this increases to at least 6% using their note added in proof), which would indicate that these systems are considerably different than rich clusters (which have baryon fractions of 10%–30%) and very similar to some theoretical predictions for the baryonic content of the universe as a whole (e.g., White et al. 1993).

In order to determine whether these two groups are typical of compact groups, we assembled a large sample of X-ray

observations of HCGs. In addition to our Position Sensitive Proportional Counter (PSPC) observations of four HCGs (selected to have a large enough angular size to be resolved by the PSPC and far enough north for follow-up optical observations at the Michigan-Dartmouth-MIT [MDM] Observatory on Kitt Peak), we obtained all the archived *ROSAT* PSPC observations of HCGs available as of 1994 April (including those of HCG 62 and the NGC 2300 group). This resulted in a sample of 13 groups, which we then reduced in a uniform manner. The PSPC observations allowed us to find the fraction of groups with extended emission and then determine the mass of hot gas and the total gravitating mass of those systems. These masses were compared to the baryonic mass in the galaxies of each group in order to determine gas-to-stellar mass ratios and baryonic fractions. This study is an improvement over previous work since the flattening properties of the PSPC are better understood and the background subtraction was investigated thoroughly. In addition, the reduction and analysis was uniformly applied to all the objects, so they could be compared to one another.

2. OBSERVATIONS AND DATA REDUCTION

Four HCGs were observed with the PSPC as part of our observing program (HCG 2, 10, 68, and 93), while seven other HCGs and the NCG 2300 group has PSPC observations obtained from the *ROSAT* archives. In addition, HCG 94 can be seen in the observation of HCG 93, although it is over 30′ off-axis. A summary of the properties of the groups is in Table 1 (throughout this paper, $H_0 = 50$ km s^{-1} Mpc^{-1} and $q_0 = 0$ are assumed).

All observations were reduced in the same manner. First, we examined the background level as a function of time by binning the counts in an ~ 100 arcmin^2 region containing no apparent X-ray sources in ~ 100 s intervals. We examined the value of the signal-to-noise ratio for a source 10% as bright as the modal background level as we included time bins with greater and greater background levels. Typically, the signal-to-noise ratio would rise steadily as more bins were included, but fall for those bins at very high background levels. We then excluded all time intervals which had background levels above the point where the signal-to-noise ratio started to decrease. In all but one case (HCG 92), this entailed the exclusion of less than 8% of the total observing time. Subsequent analysis was performed using these filtered observations. Table 2 lists the total and net observing times, as well as the Galactic neutral hydrogen column (N_H) in the direction of each group as determined by Stark et al. (1992).

TABLE 2

X-RAY OBSERVATIONS OF GROUPS

Group (1)	Total Observing Time (ks) (2)	Time Used (ks) (3)	N_H (4)
HCG 2.....	20.17	20.17	4.08
HCG 4.....	9.33	9.33	1.55
HCG 10.....	16.10	16.10	5.18
HCG 12.....	10.79	10.79	4.05
HCG 44.....	4.67	4.67	2.13
HCG 62.....	19.72	19.52	2.87
HCG 68.....	14.99	14.99	1.03
HCG 79.....	5.29	4.91	3.96
HCG 92.....	20.88	13.41	7.53
HCG 93.....	16.76	16.27	5.36
HCG 94.....	(16.76)	(16.27)	5.10
HCG 97.....	13.89	13.89	3.62
N2300 group	6.04	6.04	5.95

NOTE.—Col. (4) is the Galactic neutral hydrogen column in the direction of each group, in units of 10^{20} cm^{-2}.

Each PSPC field was flattened in the appropriate energy band using the program CAST_EXP (Snowden et al. 1994), which creates more accurate flat fields than those provided by the US *ROSAT* Science Data Center, which are not energy-band specific. This program uses the aspect and event rate information for each observation, along with the time intervals used and the energy band of interest, to make a flat field. These flat fields were used to make flat images for analyzing the extent of any X-ray emission, as well as to determine normalization factors for spectral analysis. The flat images excluded any energy channels that would be absorbed heavily by the neutral hydrogen column in our Galaxy (e.g., $kT < 0.5$ keV for high columns).

In order to test the accuracy of our field flattening, we flattened three fields from the *ROSAT* archives (rp700112, rp700117, and rp700375) that had relatively few sources, none of them expected to be extended. These three fields intention-

TABLE 1

PROPERTIES OF GROUPS ANALYZED

Group (1)	z (2)	Distance (Mpc) (3)	$N_{accordant}$ (4)	Comments (5)
HCG 2	0.0144	86.3	3	Our observation
HCG 4	0.0280	168	3	Bright AGN in galaxy a
HCG 10	0.0161	96.5	4	Our observation
HCG 12	0.0485	291	5	Not well resolved, diffuse emission?
HCG 44	0.0046	27.6	4	
HCG 62	0.0137	82.1	4	Diffuse emission (Ponman & Bertram 1993)
HCG 68	0.0080	48.0	5	Our observation, diffuse emission
HCG 79	0.0145	86.9	4	Seyfert's Sextet, unresolved
HCG 92	0.0215	129	4	Stephan's Quintet, unresolved
HCG 93	0.0168	101	4	Our observation
HCG 94	0.0417	250	7	Off-axis, X-ray luminous
HCG 97	0.0218	131	5	Diffuse emission
N2300 group.....	0.0070	42.0	3	Diffuse emission (Mulchaey et al. 1993)

NOTE.—Col. (2) is the median redshift of each group, and col. (4) is the number of galaxies in each group with accordant redshifts. Both are from either Hickson 1993 or Mulchaey et al. 1993.

ally span a range of neutral hydrogen columns ($N_H = 4.07$, 1.20, and 2.10×10^{20} cm^{-2}, respectively) and exposure times (19.8, 22.7, and 13.4 ks) in order to see what effect these parameters had on the flattening. None had more than 1 ks of observing time excluded due to high background levels.

A plot of the background level as a function of distance from field center for the two high-N_H fields (rp700112 and rp700375) is shown in Figure 1. The data points are averages of annular bins 40″ wide. The background level becomes less well determined at the radius of the support ring ($r \sim 20'$) and beyond, as well as at radii less than 7′, where the targets of the observation may not be adequately excluded. Further analysis shows that the fluctuations of the background for $7' < r < 20'$ are ~ 1.4 times greater than that expected from photon statistics alone. It is unclear whether this is due to unsubtracted point sources, fluctuations in N_H, imperfections in the flattening process, or a combination of all these. Whatever the cause, this larger error should be applied when analyzing PSPC data, especially when searching for extended emission that is only a fraction of the background level.

The low-N_H field, rp700117, could not be flattened to the same degree of accuracy as the other two fields. Not only was it more difficult to create a good flat when nearly all the energy channels were included, but this field exhibited an increase in surface brightness with radius, regardless of the energy band examined (Fig. 2); especially for $r > 20'$. Even when channels with $kT < 0.5$ keV were excluded (*heavy line*), the background counts rise with radius even within the support ring. It is not clear whether this is an artifact of the flattening process or some systematics of the field or observation (or some combination of these). This demonstrates that processing PSPC images is not guaranteed to produce perfectly flat fields, with the greatest difficulties at $r \geq 20'$. Again, extreme caution must be exercised when analyzing low surface brightness X-ray features—it can be highly difficult to disentangle such features from telescope or reduction systematics.

3. ANALYSIS AND DISCUSSION

All of the spatial and the initial spectral reduction was done using the PROS package within IRAF, while the remainder of the spectral reduction used XSPEC. Our procedure was as follows: after the initial reduction outlined in § 2, a flattened image of the central square degree of the PSPC field was created, using only energy channels largely unabsorbed by neutral hydrogen in the Galaxy. The flat field from CAST_EXP was normalized so that the maximum pixel value is 1. A smoothed image (smoothed with a Gaussian with $\sigma = 16''$) was then created and viewed with an overlay of the optical galaxy positions. Contour maps of the X-ray emission of the groups with detected extended emission are in Figure 3. Each smoothed image was visually examined to see if any of the galaxies in the group have X-ray emission and/or if there is any extended X-ray emission associated with the group. If there was extended emission, we used annular binning on the unsmoothed data to determine its extent.

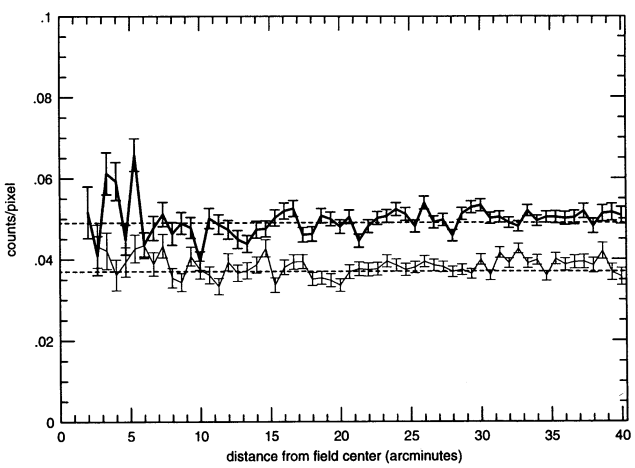

FIG. 1.—Background level as a function of distance from field center for rp700112 (*light line*) and rp700735 (*heavy line*). Each pixel is 4″ on a side. The dashed lines represent the best fit for the average for $7' < r < 20'$.

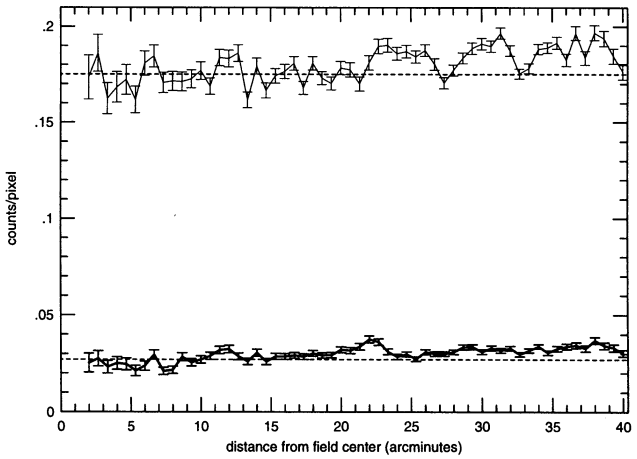

FIG. 2.—Background level as a function of distance from field center for two different flattening attempts on rp700117. Each pixel is 4″ on a side. The light line represents a full spectrum (0.1–2.2 keV) image with a soft energy flat field, while the heavy line represents an image excluding energies less than less than 0.5 keV with a hard flat field. The dashed lines are best fits for the average for $5' < r < 15'$.

All galaxies identified in the flattened and smoothed image were spectrally analyzed, as was all extended emission. A background-subtracted, vignetting-corrected spectrum of each detection was analyzed in XSPEC, where we fit an absorbed Raymond-Smith model to the data, fixing the neutral hydrogen column to the Galactic column in the direction of the group. Since the PSPC does not allow one to fit abundances very well, we fixed abundances of diffuse gas at one-half solar and galaxies at solar abundance. If the source was too faint to fit a temperature, we fixed it to be $kT = 0.5$ keV (elliptical and S0 galaxies) or 1.0 keV (spiral galaxies and diffuse emission). The fitted model then was used to find the rest-frame luminosity of the source in the XSPEC PSPC passband (0.07–3.0 keV). The diffuse emission will be discussed in § 3.3.

For galaxies in the PSPC field but not detected at the $\lesssim 3\ \sigma$ level, we determined upper limits. First, we found the net number of photons in a circular aperture of radius equal to the major-axis diameter of the galaxy, as given in Hickson (1993). Then we obtained a luminosity (if the net counts were 2 σ or greater above the background—such galaxies could be seen in the smoothed image) or a 3 σ upper limit on the luminosity for each galaxy scaling the luminosity of a well-detected galaxy of the same type in the same group by the ratio of the net counts of the two galaxies. If there was not a galaxy of the same type (E/S0 vs. spiral) in the group, we forced a fit of the appropriate temperature on a well-detected galaxy in the group and used the result to obtain a scaled luminosity. This procedure was not carried out for galaxies whose emission could not be

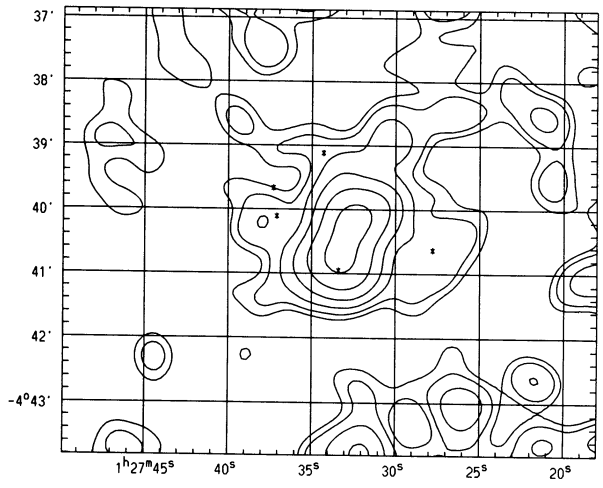

FIG. 3*a*

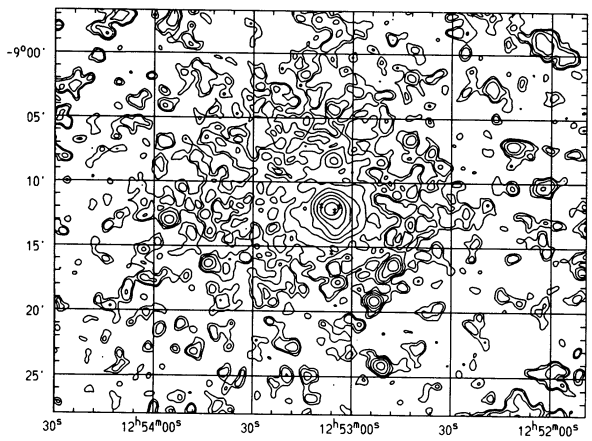

FIG. 3*b*

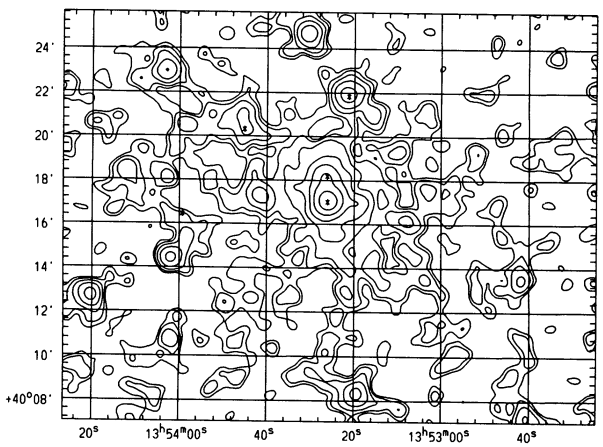

FIG. 3*c*

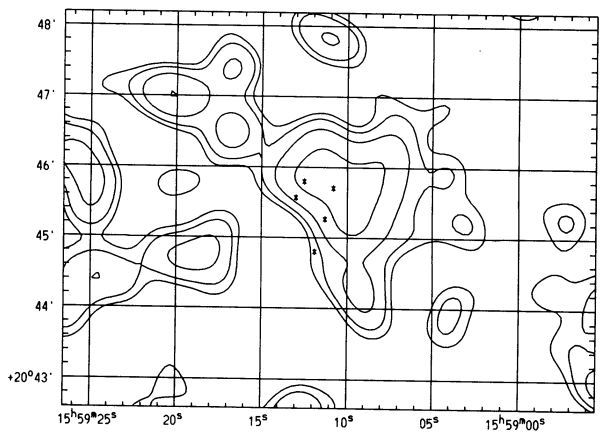

FIG. 3*d*

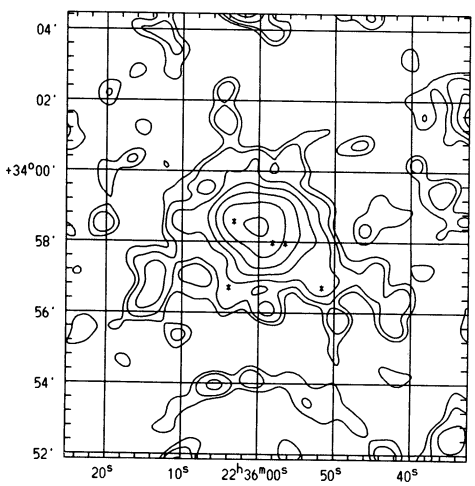

FIG. 3*e*

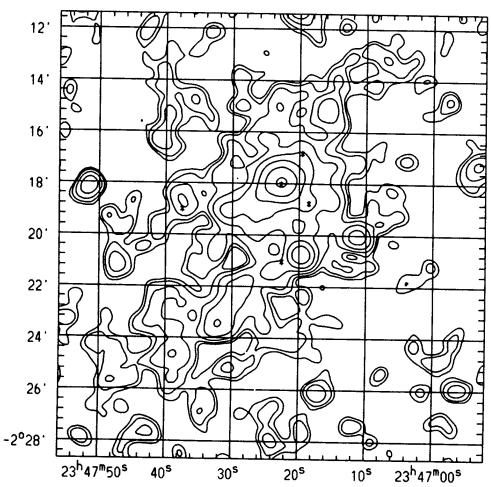

FIG. 3*f*

FIG. 3.—Contour maps of smoothed (by a Gaussian of FWHM = 0.63) X-ray emission from compact groups. Optical positions of group galaxies are marked by asterisks, and PSPC coordinates are for epoch J2000.0. Contours are drawn at 1 σ, 2 σ, 4 σ, 8 σ, ..., above the background level, where σ is calculated for the smoothed background. (*a*) HCG 12. (*b*) HCG 62. (*c*) HCG 68. (*d*) HCG 79. (*e*) HCG 92. (*f*) HCG 97. (*g*) NGC 2300 group.

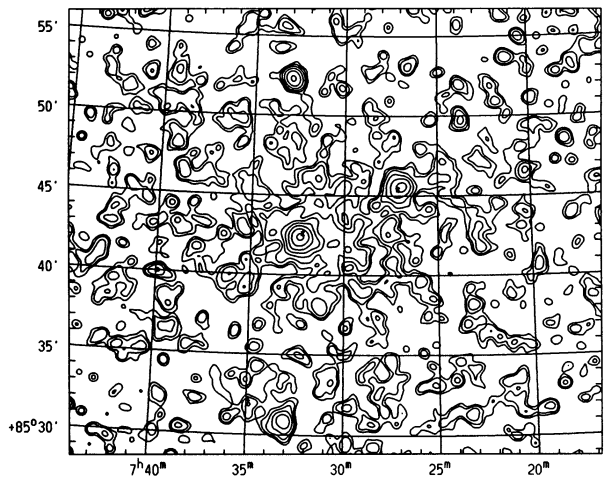

FIG. 3g

separated from nearby bright emission (e.g., the galaxies of HCG 4). Table 3 summarizes the X-ray and optical properties of all PSPC-detected compact group galaxies. We use the galaxy designations of Hickson (1982, 1993) throughout this paper.

TABLE 4

BASIC PROPERTIES OF EXTENDED EMISSION

Group	Radial Extent	Background Level	Net Counts
HCG 12	2'.2 (0.19 Mpc)	0.014	96 ± 23
HCG 62	15 (0.36 Mpc)	0.080	3603 ± 318
HCG 68	9 (0.13 Mpc)	0.098	710 ± 88
HCG 79	...	0.012	28.4 ± 11.1
HCG 92	3.0 (0.11 Mpc)	0.040	501 ± 56
HCG 97	7 (0.27 Mpc)	0.026	923 ± 78
N2300 group.....	17 (0.21 Mpc)	0.0086	838 ± 131

NOTE.—Col. (2) is the radial extent of the emission as discussed in § 3.3, and col. (4) is the background level in counts per (4" × 4") pixel.

3.1. *Individual Groups: Comments*

Eight of the 13 groups we analyzed have detectable extended X-ray emission (Table 4). Unfortunately, several of the groups are not completely resolved with the PSPC (which has an FWHM of 25")—it was impossible to separate diffuse emission from emission from the galaxies. Also, some of the same groups had observing times that were too short to obtain high signal-to-noise ratio detections of the extended emission. Only four groups had resolved detections of diffuse X-ray gas in the potential well of the group. The observations of each of the 13 groups are discussed more thoroughly below.

TABLE 3

GROUP GALAXIES DETECTED IN X-RAYS AND UPPER LIMITS

Galaxy (1)	Name (2)	Type (3)	M_B (4)	kT (keV) (5)	Net Counts (6)	L_X (7)
HCG 2a	UCG 312	SBd	−21.4	1	78 ± 12	2.4
HCG 2b	Mrk 552	Sp?	−20.3	1	47 ± 10	1.8
HCG 2c	UCG 314	SBc	−20.6	1	10.7 ± 5.1	0.32
HCG 4a		Sc	−22.6	AGN	3153 ± 64	1.13×10^3
HCG 10a	NGC 536	SBb	−22.3	1	64 ± 16	3.1
HCG 10b	HGC 529	E1	−22.2	0.5	59 ± 12	2.9
HCG 10c	NGC 531	Sc	−20.8	1	<21.5	<1.0
HCG 10d	NGC 542	Scd	−20.2	1	<10.6	<0.51
HCG 44a	NGC 3190	Sa	−20.7	1	52 ± 13	0.61
HCG 44b	NGC 3193	E2	−20.6	0.5	72 ± 16	0.69
HCG 44c	NGC 3185	SBc	−19.7	1	27 ± 12	0.34
HCG 44d	NGC 3187	Sd	−19.1	1	22.4 ± 6.5	0.28
HCG 62a	NGC 4761	E3	−21.2	0.87 ± 0.01	5067 ± 80	199[a]
HCG 62b	NGC 4759	S0	−20.8	...	...	...
HCG 62c	NGC 4764	S0	−19.0	...	...	...
HCG 68a	NGC 5353	S0	−21.6	0.62 ± 0.10	717 ± 29	10.6[b]
HCG 68b	NGC 5354	E2	−21.2	...	...	...
HCG 68c	NGC5350	SBbc	−21.5	1	119 ± 15	1.5
HCG 68d	NGC 5355	E3	−19.7	0.5	94 ± 15	0.75
HCG 68e	NGC 5358	S0	−19.2	0.5	<25.4	<0.20
HCG 93a	NGC 7550	E1	−22.4	0.5	41 ± 15	2.2
HCG 93b	NGC 7549	SBd	−21.8	1	14.4 ± 5.6	1.2
HCG 93c	NGC 7547	SBa	−21.1	1	15.9 ± 5.3	1.3
HCG 93d		S0	−19.7	0.5	<13.5	<0.73
HCG 97a	IC 5357	E5	−21.4	1.04 ± 0.09	395 ± 22	56.6[c]
HCG 97b	IC 5359	Sc	−20.8	1	<66.5	<9.5
NGC 2300.....		E3	−21.3	0.50 ± 0.12	301 ± 19	9.1
NGC 2276.....		Sc	21.4	1.0 ± 0.4	98 ± 12	3.1
IC 455		S0	−19.1	0.5	<15.7	<0.47

NOTE.—Col. (3) is the Hubble type of each galaxy from either Hickson 1993 or Mulchaey et al. 1993; col. (4) is its absolute blue magnitude as determined from the group distance (Table 1) and its apparent blue magnitude in Hickson 1993; col. (7) is the fitted X-ray luminosity in units of 10^{40} ergs s^{-1} for the 0.07–3.0 keV energy band.

[a] The X-ray temperature and luminosity for HCG 62a, 62b, and 62c are for a region 3' in radius centered on 62a—the individual galaxies are not resolved.

[b] HCG 68a and 68b are not resolved separately, so the X-ray temperature and luminosity given are for both galaxies.

[c] The X-ray temperature and luminosity for HCG 97a are for a region centered on the galaxy and 48" in radius.

HCG 2.—All three of the galaxies in this group with accordant redshifts are detected in X-rays, but no extended emission is seen.

HCG 4.—A bright power-law source in galaxy a of this group overwhelms any possible signal from other sources in the group. This source has a power-law index $\alpha = 2.08 \pm 0.04$ (where the emission depends on the energy as $E^{-\alpha}$) and a luminosity in the PSPC passband of 1.1×10^{43} ergs s^{-1}. Galaxy a was found to contain a possible active galactic nucleus (AGN) in the Montreal Blue Galaxy Survey (Coziol et al. 1993), and this observation appears to confirm the presence of an active nucleus in that galaxy.

HCG 10.—Two of the four galaxies in this group (a and b) are well detected by the PSPC, but no extended emission is seen.

HCG 12.—This quintet of galaxies is not resolved with the PSPC. The emission is extended, but the 25″ resolution of the instrument is not sufficient to separate galaxy emission from diffuse emission.

HCG 44.—This group has three (a, b, and c) of its four galaxies clearly detected in the PSPC observation, but there is no extended emission.

HCG 62.—HCG 62 contains two central, X-ray–bright early-type galaxies as well as very strong diffuse X-ray emission. It was first analyzed by Ponman & Bertram (1993).

HCG 68.—This group is the only one of our four original PSPC observations to show diffuse emission. Four (a–d) of the five galaxies in the group are well detected, although the emission from galaxies a and b overlaps and cannot be resolved separately.

HCG 79.—This group is better known as Seyfert's Sextet. Since it is a very dense, elliptical-rich group, it might well be expected to be a strong source of X-ray emission; unfortunately, the usable time for this observation was so short (4.9 ks) that there were not enough photons detected to perform any spectral analysis. In addition, the galaxies in the group are too close together to be individually resolved with the PSPC even if the observation time were sufficiently long.

HCG 92.—The PSPC observation of this group (better known as Stephan's Quintet) presented some difficulties in reduction. Not only are the galaxies too close together to be resolved individually by the PSPC, but 36% of the original observing time needed to be discarded because the background level was too high. Nonetheless, this group has a strong X-ray detection, though it is unclear whether it is diffuse emission or unresolved emission from individual galaxies.

HCG 93.—Only galaxy a of this group is clearly detected in the PSPC observation—no extended emission is seen.

HCG 94.—Serendipitously, this group is seen in the observation of HCG 93 (it is 30.5 away from HCG 93). Because it is so far off-axis, no determination can be made about the spatial structure of the X-ray emission, but some spectral analysis can be done (§ 3.3.6).

HCG 97.—This group has fairly bright extended emission surrounding galaxy a, making it difficult to detect or set upper limits on the emission from any of the individual galaxies of the group. Even for galaxy a, we were forced to assume that all the emission from it was within a radius of 48″ of the center, which may not give an accurate picture of its X-ray properties.

NGC 2300 group.—We take this group as consisting of three galaxies: NGC 2300 (E3, $M_B = -21.3$), NGC 2276 (Sc, $M_B = -21.4$), and IC 455 (S0, $M_B = -19.1$). This is the same grouping as used by Mulchaey et al. (1993), who did the first analysis of the X-ray properties of this group.

3.2. *Properties of Group Galaxies*

One question that can be addressed with this sample of compact group galaxies is whether the apparently very dense environment of these groups produces systematic differences in the X-ray to optical luminosity relation. Such relations have been determined from *Einstein* observations of field galaxies and can be easily translated to the *ROSAT* passband. Bregman, Hogg, & Roberts (1992, hereafter BHR) find a relation for early-type galaxies of $L_X \sim L_B^{2.4}$, and although the picture for spiral galaxies is less clear, L_X appears to be linearly correlated with the number of Population I stars in a galaxy and thus with L_B (Fabbiano & Trinchieri 1985).

We have examined the L_X-L_B relation for all of the galaxies detected in the X-ray in our sample that were not contaminated by diffuse emission or overlapping galaxy emission (questionable cases are noted below and in Table 3). Blue luminosities were found using the blue apparent magnitudes in Hickson (1993), which have been corrected for overlap from nearby galaxies. Both the spiral and the early-type galaxies in our sample appear to follow the field galaxy L_X-L_B relations, with a few exceptions (Fig. 4). The late-type galaxies follow a linear relation quite closely; HCG 2b (at $\log L_B = 10.3$, $\log L_X = 40.2$) is somewhat overluminous in X-rays for its blue luminosity, but it is Markarian galaxy and thus may be undergoing some unusual activity. Among the early-type galaxies, HCG 97a is the galaxy with the highest L_X and falls about an order of magnitude above the BHR relation, but this galaxy was difficult to resolve from the diffuse emission in its group, and its intrinsic emission may be less than our stated value. HCG 44b also falls an order of magnitude above the BHR relation, but has one of the lowest blue luminosities in the sample; in the opposite sense, the two elliptical galaxies with the highest blue luminosities (HCG 10b and HCG 93a) fall over an order of magnitude below the early-type L_X-L_B relation. None of these three groups (HCG 10, 44, and 93) has extended emission, so confusion is not an issue. HCG 44b and HCG 10b have no known pecularities, and although HCG 93a is a shell galaxy (Pildis & Bregman 1995), there is no reason to

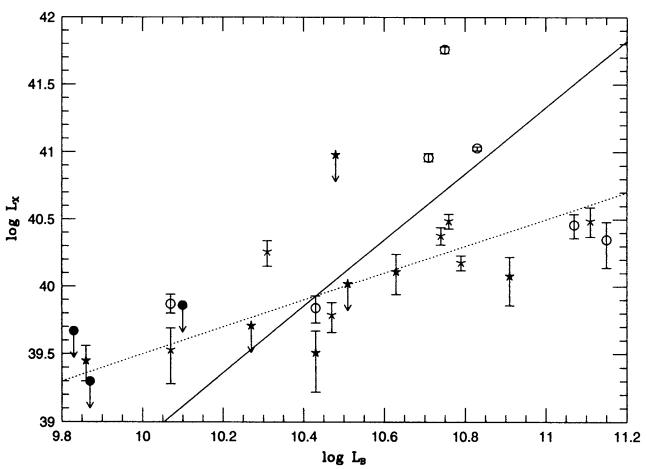

FIG. 4.—Optical to X-ray luminosities for galaxies in compact groups. Open circles denote early-type galaxies with strong detections, and filled circles are early-type galaxies with weak detections; asterisks are late-type galaxies with strong detections, and stars are late-type galaxies with weak detections. Error bars are from the error in the net counts, as listed in Table 3. Upper limits on the X-ray luminosity are denoted by symbols with descending arrows. The L_X-L_B relation for early-type galaxies of BHR, converted to the *ROSAT* passband, is shown as a solid line; a linear relation appropriate for late-type galaxies is shown as a dotted line.

expect a relation between optical fine structure and X-ray luminosity. These results may indicate that early-type galaxies in compact groups have a flatter L_X-L_B relation than do field galaxies, although this sample is too small to address this issue definitely.

3.3. *Properties of Groups with Extended Emission*

For the eight groups in which extended X-ray emission was detected, we determined the total gravitating mass of the group, the hot gas mass, the gas-to-stellar mass ratio, and the baryonic fraction, if possible. Four of the groups in our survey (HCG 62, 68, and 97, and the NGC 2300 group) are at least partially resolved with the PSPC, and so the masses obtained for those groups are the most credible. Three groups (HCG 12, 79, and 92) are unresolved (also, HCG 79 is less than 3 σ detection), and the observation of HCG 94 is too far off axis to determine the spatial profile of its emission.

In this analysis, all point and slightly extended sources in the PSPC field (stars, group galaxies, etc.) were masked off, and then the center of the emission was determined by assuming that the emission was symmetrically distributed. As can be seen in Figure 3, the extended emission in these groups appears fairly symmetrical, which implies that the gas has had time to relax into the group potential. The elongation seen in the X-ray isophotes of some groups (notably HCG 97) may be due to a somewhat unrelaxed potential, but this level of disturbance will create only a 20% uncertainty in the calculated mass, according to recent simulations (Evrard, Metzler, & Navarro 1995).

The background level and maximum extent of the emission was determined by examining the radial profile of the emission (see Figs. 5–9) and the background level. All of these groups have a radial extent of X-ray emission of over 1′, and none has a bright central point source. Since the point-spread function of the PSPC at energies of 0.5–1.0 keV falls to less than 10^{-3} of its central value for radii greater than 1′ (Hasinger et al. 1992), the PSF does not affect our determination of the background level or the radial extent of the emission.

We fit the radial surface brightness profile with a convolution of the point-spread function of the PSPC with the standard hydrostatic-isothermal beta model (Cavaliere & Fusco-Femiano 1976):

$$S(r) = S_0\left[1 + \left(\frac{r}{r_{\rm core}}\right)^2\right]^{-3\beta+0.5},$$

where S_0, $r_{\rm core}$, and β are free parameters. This model, along with the spectral fit for each group (see Table 5), allows one to solve for the gas mass and, again assuming hydrostatic equlibrium, for the gravitating mass interior to the radius r:

$$M(r) = -\frac{kT(r)r}{\mu m_p G}\left(\frac{d\ln\rho_{\rm gas}}{d\ln r} + \frac{d\ln T}{d\ln r}\right),$$

where the first derivative equals -3β and the second is assumed to be zero for all groups except for HCG 62 (which is the only group bright enough for us to measure the temperature gradient). In galaxy clusters (and HCG 62), the temperature gradient is small compared to 3β, so our assumption of isothermality does not have a large effect on the determination of $M(r)$. The stellar mass in galaxies was determined by assuming a mass-to-light ratio of $M/L_B = 8$ in solar units. The mass-to-light ratio for galaxies in these groups certainly will vary by Hubble type and interaction history (Rubin et al. 1991; White et al. 1993; Worthey 1994), and the average value for a group may be as low as $M/L_B = 3$, but we will use a single uniform ratio for the sake of simplicity and easy comparison.

The determination of the gaseous mass of these systems is sensitive to the abundance used, a quantity that usually cannot be obtained securely from these data. The reason that the gas mass depends upon the metallicity is that line emission can be the main contributor to the X-ray spectrum at $kT \sim 1$ keV, so the inferred emission measure increases as one adopts lower abundances. For example, when fixing all other parameters in a spectral fit, the emission measure rises by up to a factor of 2 as the abundance is decreased from solar values to half-solar. As the mass is proportional to the square root of the emission measure, uncertainties in the abundance can lead to inaccuracies in the gas mass determination of up to 50%.

Another source of uncertainty in the gas mass estimate can be traced to the background level used when fitting a beta model to the system. If the background level is taken to be less than the true background, then the diffuse emission appears to extend further in radius and has a shallower slope (lower value of β). The gas mass estimate is increased by the larger radius and, to a lesser extent, by the smaller beta value. In extreme cases, this can lead to a factor of 2 difference in the implied gas mass. The group with the most uncertain background level is HCG 62, which may have a background 10% lower than the level we chose. The effect of this difference on our calculated quantities is discussed extensively in § 3.3.2. The remaining groups have much better determined backgrounds (see Figs. 5–9).

The gravitational mass is considerably less sensitive to the

TABLE 5

FITTED SPECTRAL AND SPATIAL PROPERTIES OF DIFFUSE EMISSION

Group (1)	kT (keV) (2)	VEM (3)	n_0 (cm^{-3}) (4)	β (5)	$r_{\rm core}$ (arcmin) (6)	L_X (7)
HCG 12	0.72 ± 0.36	0.57 ± 0.85	5.7×10^{-3}	$0.92^{+0.44}_{-0.11}$	$0.52^{+0.10}_{-0.20}$	8.27
HCG 62[a]	[b]	43.2 ± 2.8	1.5×10^{-3}	0.512 ± 0.015	2.46 ± 0.15	19.5
HCG 68	0.98 ± 0.13	3.4 ± 1.3	1.3×10^{-3}	0.61 ± 0.04	$2.25^{+0.30}_{-0.20}$	1.21
HCG 97[c]	0.97 ± 0.11	5.9 ± 1.5	6.0×10^{-3}	$0.480^{+0.010}_{-0.015}$	0.22 ± 0.05	13.2
N2300 group.....	0.93 ± 0.20	13.1 ± 4.4	2.8×10^{-4}	0.321 ± 0.015	$2.19^{+0.35}_{0.30}$	2.92

NOTE.—Col. (3) is the volume emission measure divided by $4\pi D^2$ (where D is the distance to the group) in units of 10^{10} cm^{-5}; col. (4) is the central gas density; col. (5) is the fitted value of β; col. (6) is the fitted value of the core radius; col. (7) is the fitted X-ray luminosity in units of 10^{41} ergs s^{-1} for the 0.07–3.0 keV energy band.

[a] Excludes all emission within a radius of 3′ of the central galaxies.

[b] This group has a measurable temperature gradient—see the text.

[c] Excludes all emission within a radius of 48″ of the central galaxy.

TABLE 6

COMPONENT MASSES FOR COMPACT GROUPS

Group (1)	$M_{grav}/M_\odot$ (2)	$M_{gas}/M_\odot$ (3)	Stellar Mass $(M_*/M_\odot)$ (4)	M_{gas}/M_* (5)	f_{baryon} (6)
HCG 2	...	$<3.8 \times 10^{10}$	8.3×10^{11}	<4.6%	...
HCG 4[a]	...	...	1.8×10^{12}	...	...
HCG 10	...	$<4.4 \times 10^{10}$	2.4×10^{12}	<1.8	...
HCG 12[b]	1.4×10^{13}	2.2×10^{11}	1.9×10^{12}	12	15%
HCG 44	...	$<2.2 \times 10^{10}$	6.0×10^{11}	<3.7	..
HCG 62	2.9×10^{13}	8.1×10^{11}	7.3×10^{11}	110	5.3
HCG 68	8.7×10^{12}	4.0×10^{10}	1.6×10^{12}	2.5	19
HCG 79	...	3.5×10^{10}	6.3×10^{11}	5.5	...
HCG 92	...	...	3.5×10^{12}	...	...
HCG 93	...	$<5.4 \times 10^{10}$	2.2×10^{12}	<2.5	...
HCG 97	1.4×10^{13}	1.5×10^{11}	1.5×10^{12}	10	12
N2300 group.....	7.0×10^{12}	5.2×10^{10}	9.2×10^{11}	5.7	14

NOTE.—Col. (2) is the gravitating mass in solar masses; col. (3) is the gas mass in solar masses; col. (4) is the stellar mass in solar masses assuming $M/L_B = 8$; col. (5) is the ratio of gas mass to stellar mass; col. (6) is the baryon fraction (gas mass plus stellar mass, divided by the gravitating mass).

[a] The AGN in HCG 4a is too bright to allow an estimate of an upper limit on the gas mass.

[b] M_{gas} may to be too large and M_{grav} may not be well determined because of spatial confusion between galaxy emission and the diffuse group emission.

background level than is the gas mass. If the background level is underestimated and thus β is smaller and the extent r_{max} is larger, the gravitational mass changes only slightly, since $M_{grav} \sim \beta r_{max}$. The choice of abundance does have some effect on the gravitational mass since it is also proportional to the temperature of the gas. Lowering the abundance from solar to half-solar values will raise the fitted temperature, and thus M_{grav}, by 10%–20%.

For the groups with nondetections or very poor detections of X-ray emission, we found upper limits on the amount of hot gas. After finding the net number N of photons within a circle of radius r_a (the radius of each group as given by Hickson 1982) and the rms error σ, we scaled the normalization factor of a 1 keV source (fitted with an abundance of half the solar value) in the same field by the ratio of $N + 3\ \sigma$ (if $N > 0$) or $3\ \sigma$ (if $N \leq 0$) to the net counts of that 1 keV source. From that scaled normalization, and assuming that $\beta = 0.5$, that the radial extent of the emission is 0.2 Mpc, and that r_{core} is 1/6 the radius of the emission (along with the assumption that the temperature of the emission is 1 keV, all conservative guesses given the results we found with the well-detected diffuse emission), we calculated the upper-limit gas mass. The results of these analyses are listed in Table 6 and discussed in greater detail below.

3.3.1. *HCG 12*

The emission from this group is centered at the PSPC position $1^h27^m33^s.0$, $-4°40'21''$ (throughout this paper, coordinates are for epoch J2000.0), which is north-northwest of galaxy a, halfway between galaxies d and e, and it has a radial extent of 2.2 (0.19 Mpc) (Fig. 5).

Even though the galaxies of this group are not resolved in this observation, and thus the extended X-ray emission seen may be partially or mostly emission from individual galaxies, we fit a beta model to it in order to obtain an upper limit on the gaseous mass of the group and an estimate of the total

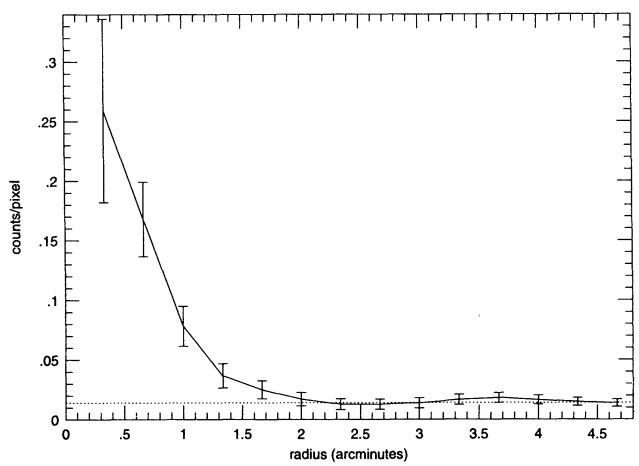

FIG. 5a

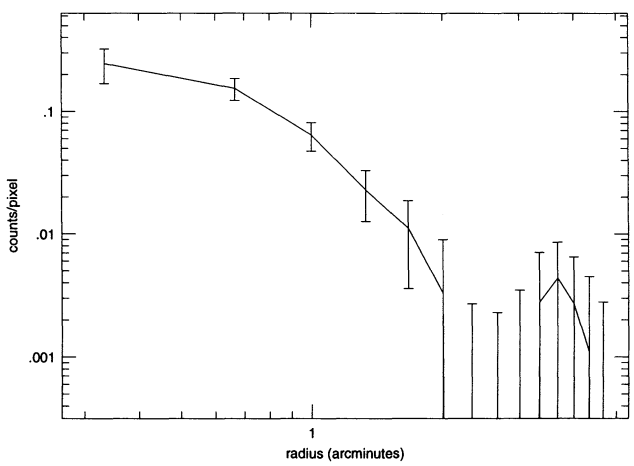

FIG. 5b

FIG. 5.—Radial profile of the extended emission in HCG 12. Each pixel is 4″ × 4″. (*a*) The linear-linear plot shows the choice of background level (*dashed line*). (*b*) Radial profile of background-subtracted emission as log counts pixel^{-1} vs. log r.

mass. Using this fit as well as the spectral fit above, we find that the total gravitating mass of this group is $1.4 \times 10^{13}\ M_\odot$, with an upper limit of $2.1 \times 10^{13}\ M_\odot$ if $\beta = 1.36$—the 1 σ upper limit (Table 5)—is used. The mass of hot gas is $2.2 \times 10^{11}\ M_\odot = 1.6\%\ M_{grav}$. The luminous mass of the galaxies in HCG 12 is $1.9 \times 10^{12}\ M_\odot = 14\%\ M_{grav}$, thus the gas-to-stellar mass ratio is 12% and the total baryon fraction is 15%. The uncertainties for these numbers are large (note the uncertainty of β in Table 5), mainly because the emission is only moderately well fit by a beta model. This is certainly due to unresolved galaxy emission being included in the fit.

3.3.2. *HCG 62*

We excluded the emission from the central galaxies (all emission less than 3′ from galaxy a—the center of the X-ray emission) when examining the spatial and spectral properties of the diffuse emission from this group. We find a different spatial profile than did Ponman & Bertram (1993, hereafter PB), obtaining a β of 0.51 ± 0.02 rather than 0.36 and a core radius of $2'.46 \pm 0'.15$ rather than 0′.5, and tracing emission only out to a radius of 15′ (0.36 Mpc) rather than their value of at least 20′ (Fig. 6). Other differences are that PB used an abundance of 0.3 times solar and a somewhat different fitting procedure than we did (their fit to the radial profile of this group gave $\beta = 0.38$ and $r_{core} = 2'.5$; they then used a more elaborate model to get the values above). We find a radial temperature decrease consistent with that of PB; $kT = 1.24 \pm 0.14$ keV foran annulus extending over radii of 3′–8′ to 1.07 ± 0.08 keV for an annulus of 8′–15′.

The total gravitating mass within a radius of 15′ is $2.9 \times 10^{13}\ M_\odot$, close to the value PB found at the same radius ($2.0 \times 10^{13}\ M_\odot$). However, we calculate a significantly smaller gas mass, $8.1 \times 10^{11}\ M_\odot$ within a radius of 15′ (2.8% M_{grav}), while they found $2.5 \times 10^{12}\ M_\odot$ within a radius of 20′. This difference may be attributable to our choice of background level (producing a large value of β and a smaller radial extent) and of a higher abundance than PB. Decreasing the abundance toward zero significantly worsens our spectral fit, but increases the gas mass up to 50%. The baryonic mass in galaxies is the same in both our and PB's analyses: $7.3 \times 10^{11}\ M_\odot$.

Since the largest difference between our analysis and PB's is the much smaller gas mass, we consequently found a smaller baryon fraction and gas-to-stellar mass ratio for HCG 62. Our gas-to-stellar mass ratio is 110%, versus PB's value of 310%, and our baryon fraction is 5.3% at a radius of 15′, while PB obtained a value of 11.7% at the same radius. This group has the largest gas-to-stellar mass ratio and the smallest baryon fraction of all the groups in our sample. In addition, our X-ray luminosity is less than that stated by PB, but given our different radial extent and our exclusion of the bright central 3′ as well as PB's luminosity being bolometric and ours being restricted to the PSPC band, this is not unexpected.

We also reanalyzed these data for a background level 10% below the level originally chosen since this is a plausible level at large radii (see Fig. 6*a*). Reducing the background level increases the radial extent of the emission to 27′ (0.64 Mpc) and nearby doubles the net counts. When we fit a beta model to these data, the values of β and r_{core} did not change substantially ($\beta = 0.48$ and $r_{core} = 2'.9$), but the fit was significantly poorer than in our original analysis. This new fit doubles the gas mass and increases the total mass by nearly 60%. Since the stellar mass remains the same, the gas-to-stellar mass ratio becomes 210% and the baryon fraction falls to 5.1%.

Because our analysis leads us to believe that the background is not well determined at large radii (§ 2), we believe that our original background level of 0.080 counts pixel^{-1} is the most reasonable. However, for systems like HCG 62 with emission at large radii, additional off-axis observations to determine the extent of the emission and the background level would be of considerable value.

3.3.3. *HCG 68*

The center of the diffuse emission is 1′.5 southwest of galaxy a. The emission is elongated toward the northeast and southwest and extends to a radius of 9′ (0.13 Mpc) (Fig. 7).

This group has the largest baryon fraction (19%) but the lowest measured gas-to-stellar mass ratio of all the groups with detected diffuse emission, which is the opposite extreme from HCG 62.

3.3.4. *HCG 79*

Although this group is only detected at the 3 σ level in its PSPC observation, the method used to find upper limits on the gas mass in groups was used to find a gas mass (see Table 6).

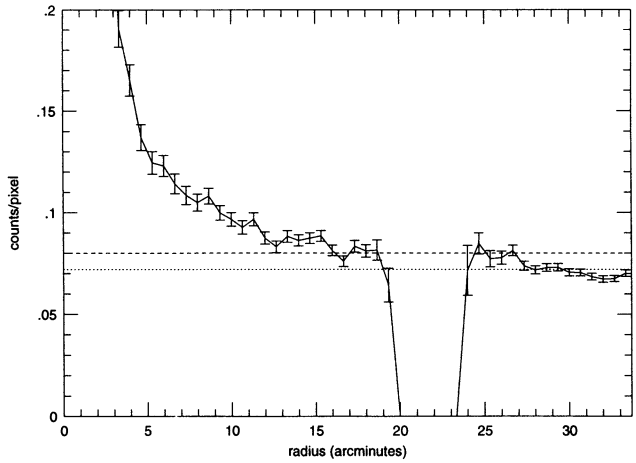

FIG. 6*a*

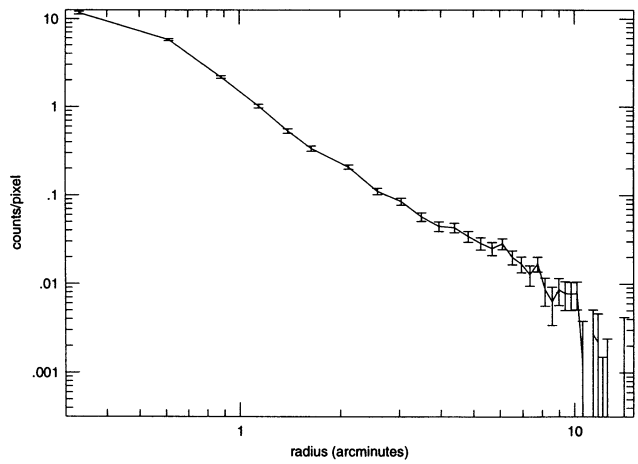

FIG. 6*b*

FIG. 6.—Radial profile of the extended emission in HCG 62. See the caption to Fig. 5. (*a*) The gap at $r \sim 20'$ is due to the exclusion of the support ring. The dashed line is the background level we chose, while the dotted line is a plausible background 10% lower. See the text for a fuller explanation.

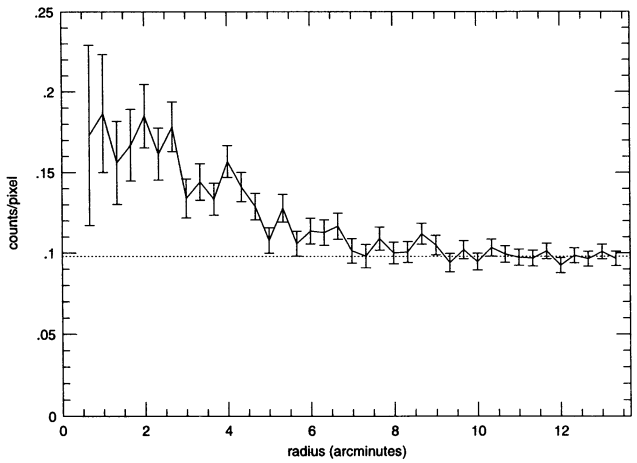

FIG. 7a

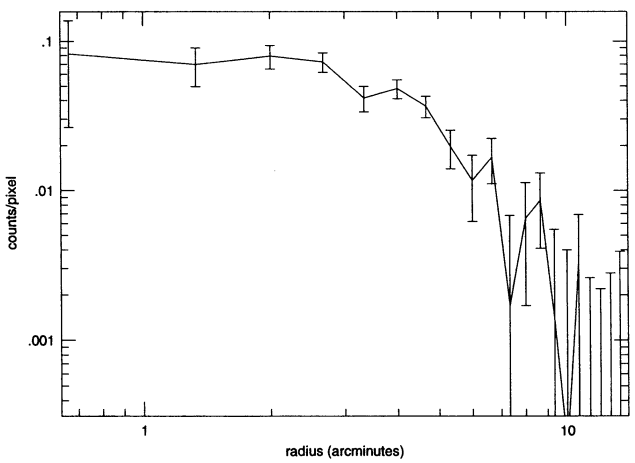

FIG. 7b

FIG. 7.—Radial profile of the extended emission in HCG 68. See the caption to Fig. 5.

Consequently, the value found is much more uncertain than those of the more X-ray–luminous groups. However, the gas-to-stellar mass ratio of 5.5% is in the same range as the other groups.

3.3.5. *HCG 92*

The center of the emission in HCG 92 is roughly halfway between galaxies b and c ($22^h36^m00^s.1$, $+33°58'23''$) and extends to a radius of 3′ (0.11 Mpc). Unfortunately, the emission of this group is very poorly fit by a beta model (the best model had a reduced χ^2 of 20.7) so we did not calculate a gas or total gravitating mass for this system. As is the case of HCG 12, a significant amount of the X-ray emission of this group is probably due to unresolved emission from the galaxies rather than diffuse hot gas in the potential well of the group. Planned HRI observations of this group should clarify the nature of the X-ray emission and allow a determination of the gas and total gravitational masses in this group.

3.3.6. *HCG 94*

HCG 94 is an extremely bright X-ray source [L(0.07–3.0 keV) = 7.19×10^{43} ergs s^{-1}] with a high temperature ($kT = 3.7 \pm 0.6$ keV) compared to other Hickson compact groups. This group may be associated with the nearby Abell cluster A2572 ($z = 0.0395$), as noted by Rood & Struble (1994). A2572 is also seen in the HCG 93 PSPC image, although it is even further off-axis than HCG 94.

3.3.7. *HCG 97*

Extended emission is centered on galaxy a and extends 7′ (0.27 Mpc) from it (Fig. 8). It is difficult to separate the emission from galaxy a from the diffuse emission, so we assumed that the diffuse emission was dominant for radii greater than 48″ (31 kpc). This radius was chosen because it is twice the optical radius (at $\mu_B = 25$ mag $arcsec^{-2}$; Hickson 1993) of HCG 97a and it is the radius outside of which the X-ray isophotes become more irregular.

3.3.8. *NGC 2300 Group*

We find that the diffuse emission in this group is centered 3′ west of NGC 2300 and that it extends 17′ (0.21 Mpc) from this point (Fig. 9), rather than the 25′ claimed by Mulchaey et al. (1993, hereafter MDMB). The emission declines quite slowly with radius ($\beta = 0.32 \pm 0.02$), and the core radius is $2.19^{+0.35}_{-0.30}$

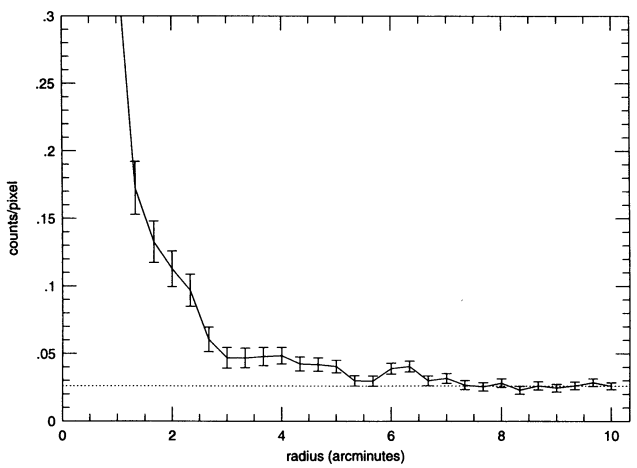

FIG. 8a

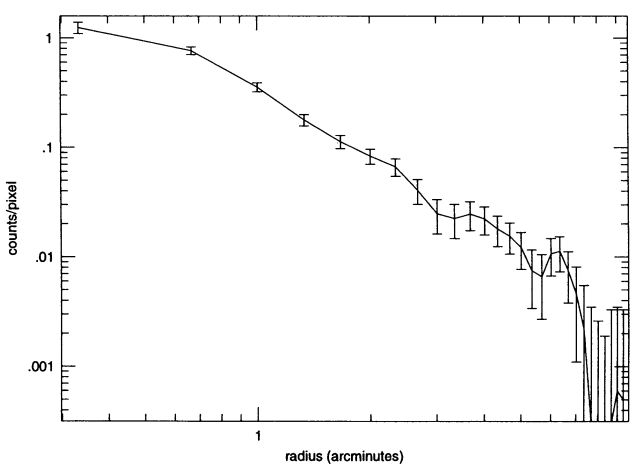

FIG. 8b

FIG. 8.—Radial profile of the extended emission in HCG 97. See the caption to Fig. 5.

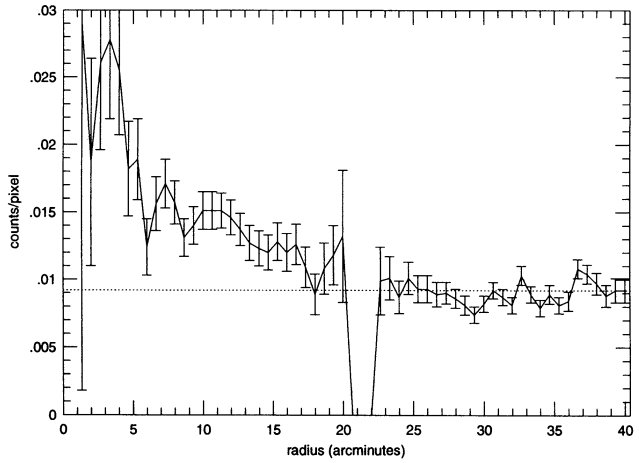

FIG. 9a

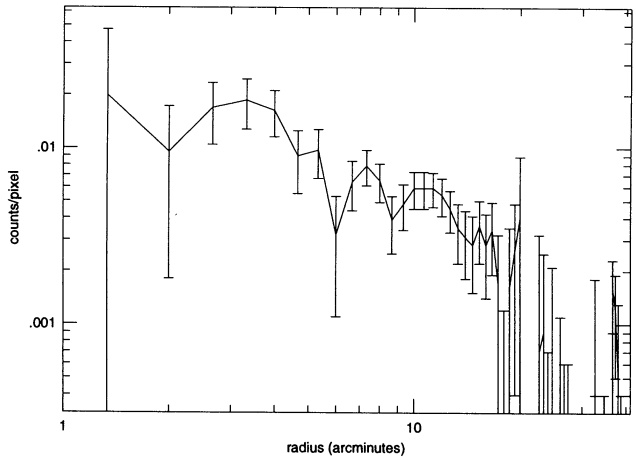

FIG. 9b

FIG. 9.—Radial profile of the extended emission in the NGC 2300 group. See the caption to Fig. 5. (*a*) The gap at $r \sim 20'$ is due to the exclusion of the support ring.

arcmin (the large uncertainty is due to the proximity of the emission from NGC 2300 to the center of the diffuse emission—a great deal of the diffuse emission is masked out along with the galaxy's emission).

We calculate a total gravitating mass for this group of $7.0 \times 10^{12}\ M_{\odot}$, over a factor of 4 less than the mass found by MDMB within a radius of 15′ and a factor of 2.9 less than the total mass they found within 25′, reported in their note added in proof. The difference between their values and ours is likely due to differences in the value of β, although this is unclear since MDMB did not publish a value of β or $r_{\rm core}$. MDMB assumed a uniform density of gas to obtain an upper limit of $5 \times 10^{11}\ M_{\odot}$ within a radius of 15′; we fit a beta model with the parameters listed above and find $M_{\rm gas} = 5.2 \times 10^{10}\ M_{\odot}$, or 0.7% of the total mass. With our standard mass-to-light ratio, the baryonic mass in the three galaxies of the group is $9.2 \times 10^{11}\ M_{\odot} = 13\%\ M_{\rm grav}$, giving a gas-to-stellar mass ratio of 5.7% and a total baryonic fraction for this group of nearly 14%, much greater than the 4% value given in MDMB. (With the corrections made in their note added in proof, however, their baryon fraction is 6%.) The disparity between our results and those of MDMB is probably related to our improved flattening and background subtraction techniques.

4. FURTHER DISCUSSION AND CONCLUSIONS

Hickson compact groups are apparently quite poor in gas as compared to richer groupings of galaxies. While larger groups and clusters have gas masses 2–6 times greater than the greater than the baryonic mass in their galaxies (Arnaud et al. 1992; David et al. 1990), all but one of the groups we analyzed have a gas-to-stellar mass ratio of less than one-eighth, with a median value of close to 5%. While this ratio is two orders of magnitude less than that found in clusters, it is somewhat higher than the 0.5%–4% values found in bright early-type galaxies (Forman, Jones, & Tucker 1985).

Even with this apparent shortage of gas relative to richer structures, these compact groups have baryon fractions in the range found in clusters and rich groups. Baryon fractions for those structures range from 10% to over 30% (Blumenthal et al. 1984; Briel, Henry, & Böringer 1992; David et al. 1994b), while the fractions for the four resolved groups in our study range from 5% to 19%. The constancy of the baryon fraction over all scales from individual galaxies to rich clusters was noted by Blumenthal et al. (1984), although more recent *ROSAT* data seem to indicate that the baryon fraction may increase with increasing mass scale (David, Forman, & Jones 1994a).

If the errors on the parameters listed in Table 5 are taken into account along with the possibility that M/L_B could be as low as 3, the gas-to-stellar mass ratio for HCG 62, the system with the largest ratio, could vary from 95% to 340% and that for HCG 68, the system with the lowest measured ratio, could be from 1.6% to 10%. The range of baryon fractions for these two groups are then 4.9%–6.4% (HCG 62) and 5.8%–24% (HCG 68). These are the largest possible errors we could calculate from our data, but these two groups—which occupy the extremes of baryon fraction and gas-to-stellar mass ration in our sample—are still fairly disinct in these two quantities. Note that the uncertainty in the abundance is not taken into account above; changing the abundance by a factor of 2 can change the gas mass by up to a factor of 50%, as noted in § 3.3.

It is important to keep in mind that comparisons between these groups, rich clusters, and individual galaxies involve properties measured at different density contrasts. The mean densities inferred from the binding mass estimates in Table 6 represent enhancements by factors greater than 2000 over the mean background density (assuming $\Omega_0 \leq 1$). For rich clusters, the mean density within an Abell radius is roughly an order of magnitude smaller, while the density contrast within a few optical radii of a large elliptical can be an order of magnitude larger. It is not unreasonable to expect that properties such as the gas-to-stellar mass ratio will vary as a function of radius from the group center or, equivalently, mean density contrast.

One concern then is that the low gas-to-stellar mass ratio may be biased by the selection on optical compactness in Hickson's catalog. More gas may lie well beyond the optical extent of the group. For a value of $\beta = 0.5$, characteristic of these groups, the gas mass is proportional to $r^{1.5}$, while the stellar mass would increase linearly with the radius if it possesses an isothermal distribution as do clusters. At the absolute extreme, the detected galaxies could be the only galaxies in the group, in which case the stellar mass is constant with radius. Under these assumptions, and if the group extends to 1 Mpc

(representing a density contrast of $\sim 10^2$), the gas-to-stellar mass ratio would increase by a factor of 3–10. Even with the largest increase, the median value of this ratio would rise from about 5% to 50%, still an order of magnitude less than that found in clusters of galaxies (David et al. 1990). Since most of the baryons are from stars in the group galaxies, changes in the baryon fraction from this effect will be minor.

Physical explanations for the low gas fractions include very efficient star formation in these systems or expulsion of ambient gas through galactic winds generated by bursts of star formation. Accurate determination of the metallicity in the gas would be a valuable diagnostic. The gas-to-stellar mass ratio could also be increased if it were determined that some of the galaxies were projected interlopers. As discussed below, this is probably not a large effect for the spiral-poor groups we find to possess detectable, diffuse emission.

Some of the groups in our sample may be superpositions of field or loose poor-group galaxies rather than bound entities. While Hickson & Rood (1988) claim that only $\sim 1\%$ of HCGs should be chance alignments, Mamon (1986) holds that roughly half are change alignments within larger poor groups, and Hernquist, Katz, & Weinberg (1994) suggest that HCGs may be portions of galaxy filaments seen end-on. An intermediate hypothesis (Sulentic 1987; Diaferio, Geller, & Ramella 1994) posits that they are entities newly (and continuously) formed within poor groups and that three-fourths are bound systems. Of the five groups (38% of our sample) that have no evidence for extended X-ray emission, all contain galaxies with morphological and/or kinematical pecularities that strongly indicate interactions (Mendes de Oliveira & Hickson 1994). This may only indicate interactions between members of a loose group that are not bound to one another, but it would be rash to declare all undetected groups unbound. Since the emission measure is proportional to the square of the gas density, a small decrease in the gas density would make a group undetectable with the PSPC. The eight groups that have extended emission are more likely to be bound, especially those that are resolved into separate diffuse and galaxy X-ray emission by the PSPC. The two highly luminous groups HCG 62 and 94 may be evolving into the cores of poor clusters or groups.

One piece of evidence that may discriminate between bound groups and superpositions is the correlation we have found between extended X-ray emission and low spiral fractions. Five of the 13 groups in our sample have spiral fractions of 50% or greater, and only one of them (HCG 92) has a possible detection of diffuse X-ray emission (note, however, that the extended emission of HCG 92 was not well fit by a beta model, indicating that emission from galaxies may be dominant). Of the eight groups with spiral fractions under 50%, seven groups have extended emission and the eighth, HCG 4, contains a bright AGN whose X-ray emission overwhelms any possible diffuse emission. This is similar to the results of Henry et al. (1995) on X-ray–selected groups: such groups have spiral fractions a factor of 2 smaller than optically selected groups. Hernquist et al. (1994) also suggest that spiral-rich HCGs may be projections, while groups rich in early-type galaxies may be bound groups. As more PSPC and HRI observations of HCGs enter the archives, this negative correlation between spiral fraction and diffuse X-ray emission can be tested more thoroughly.

HCG 62 appears to be a different object from the other groups in this study. (HCG 94 may be a similar group, but our observation of it is spatially unresolved. An on-axis PSPC observation of this group has been performed, and an HRI observation is planned; both should be enlightening.) Not only is HCG 62 very luminous in X-rays with highly extended emission, but it also has the highest gas-to-stellar mass ratio by over a factor of 9 and the lowest baryon fraction by over a factor of 2. As Ponman et al. (1994) noted, the newly discovered fossil galaxy group RX J1340.6+4018 has X-ray properties very similar to those of HCG 62. However, HCG 62 is not exceptional in its optical properties—its two central early-type galaxies overlap but do not show clear signs of interaction or merging (Pildis & Bregman 1995). Thus, X-ray–bright, gravitationally bound compact groups may not be found easily in optical surveys, and X-ray surveys may find as yet unrecognized bound galaxy groupings.

This material is based upon work supported under a National Science Foundation Graduate Fellowship and NASA grant NAGW-2135. We thank S. Snowden for the use of his CAST_EXP program and his patient help with its installation, and J. Turner and G. Rohrbach for their similar patience with the installation of PROSCON. We also acknowledge discussions with P. Hickson, L. David, R. Mushotzky, J. Mulchaey, and D. Davis. This research has made use of the NASA/IPAC Extragalactic Database (NED) which is operated by the Jet Propulsion Laboratory, Caltech, under contract with the National Aeronautics and Space Administration, as well as the Einstein On-Line Service, Smithsonian Astrophysical Observatory.

REFERENCES

Arnaud, M., Rothenflug, R., Boulade, O., Vigroux, L., & Vangioni-Flam, E. 1992, A&A, 254, 49
Bahcall, N. A., Harris, D. E., & Rood, H. J. 1984, ApJ, 284, L29
Blumenthal, G. R., Faber, S. M., Primack, J. R., & Rees, M. J. 1984, Nature, 311, 517
Bregman, J. N., Hogg, D. E., & Roberts, M. E. 1992, ApJ, 387, 484 (BHR)
Briel, U. G., Henry, J. P., & Böringer, H. 1992, A&A, 259, L31
Cavaliere, A., & Fusco-Femiano, R. 1976, A&A, 49, 137
Coziol, R., Demers, S., Peña, M., Torres-Peimbert, S., Fontaine, G., Wesemael, F., & Lamontagne, R. 1993, AJ, 105, 35
David, L. P., Arnaud, K. A., Forman, W., & Jones, C. 1990, ApJ, 356, 32
David, L. P., Jones, C., & Forman, W. 1994a, in AIP Conf. Ser., 313, The Soft X-Ray Cosmos, ed. E. M. Schlegel & R. Petre (New York: AIP), 178
David, L. P., Jones, C., Forman, W., & Daines, S. 1994b, ApJ, 482, 554
Diaferio, A., Geller, M. J., & Ramella, M. 1994, AJ, 107, 868
Evrard, A. E., Metzler, C. A., & Navarro, J. N. 1995, in preparation
Fabbiano, G., & Trinchieri, G. 1985, ApJ, 296, 430
Fasano, G., & Bettoni, D. 1994, AJ, 107, 1649
Forman, W., Jones, C., & Tucker, W. 1985, ApJ, 293, 102
Hasinger, G., Turner, T. J., George, I. M., & Boese, G. 1992, OGIP Calibration Memo CAL/ROS/92-001
Henry, J. P., et al. 1995, ApJ, submitted
Hernquist, L., Katz, N., & Weinberg, D. H. 1994, preprint
Hickson, P. 1982, ApJ, 255, 382
———. 1993, Astrophys. Lett. Comm., 29, 1
Hickson, P., Mendes de Oliveira, C., Huchra, J. P., & Palumbo, G. G. C. 1992, ApJ, 399, 353
Hickson, P., Menon, T. K., Palumbo, G. G. C., & Persic, M. 1989, ApJ, 341, 679
Hickson, P., & Rood, H. J. 1988, ApJ, 331, L69
Huchra, J. P., & Geller, M. J. 1982, ApJ, 257, 423
Mamon, G. A. 1986, AJ, 307, 426
Mendes de Oliveira, C., & Hickson, P. 1994, ApJ, 684
Moles, M., del Olmo, A., Perea, J., Masegosa, J., Márquez, I., & Costa, V. 1994, A&A, 285, 404
Moore, B., Frenk, C. S., & White, S. D. M. 1993, MNRAS, 261, 827
Mulchaey, J. S., Davis, D. S., Mushotzsky, R. F., & Burstein, D. 1993, ApJ, 404, L9 (MDMB)
Pildis, R. A., & Bregman, J. N. 1995, in preparation
Ponman, T. J., Allan, D. J., Jones, L. R., Merrifield, M., McHardy, I. M., Lehto, H. J., & Luppino, G. A. 1994, Nature, 369, 462
Ponman, T. J., & Bertram, D. 1993, Nature, 363, L51 (PB)

Rood, H. J., & Struble, M. F. 1994, PASP, 106, 413
Rubin, V. C., Hunter, D. A., & Ford, W. K. 1991, ApJS, 76, 153
Shostak, G. S., Sullivan, W. T., & Allen, R. J. 1984, A&A, 139, 15
Snowden, S. L., McCammon, D., Burrows, D. N., & Mendenhall, J. A. 1994, ApJ, 424, 714
Stark, A. A., Gammie, C. F., Wilson, R. W., Bally, J., Linke, R. A., Heiles, C., & Hurwitz, M. 1992, ApJS, 79, 77
Sulentic, J. W. 1987, ApJ, 322, 605
Sulentic, J. W., & de Mello Rabaça, D. F. 1993, ApJ, 410, 520
White, S. D. M., Navarro, J. F., Evrard, A. E., & Frenk, C. S. 1993, Nature, 366, 429
Williams, B. A., McMahon, P. M., & van Gorkom, J. H., 1991, ApJ, 101, 1957
Williams, B. A., & Rood, H. J. 1987, ApJS, 63, 265
Williams, B. A., & van Gorkom, J. H. 1988, AJ, 95, 352
Worthey, G. 1994, ApJS, 95, 107
Zepf, S. E., & Whitmore, B. C. 1993, ApJ, 418, 72